Amyloid-Induced Aggregation and Precipitation of Soluble Proteins: An Electrostatic Contribution of the Alzheimer's β(25−35) Amyloid Fibril

Takashi Konno*

Department of Physiology, Fukui Medical University, Yoshida, Fukui, 910-1193, Japan

Received September 13, 2000; Revised Manuscript Received December 12, 2000

ABSTRACT: Amyloid-induced aggregation and precipitation of soluble proteins were investigated in vitro using the amyloid fibrils of the β(25−35) peptide, a cytotoxic fragment of the Alzheimer's β-peptide at positions 25−35. The aggregation rate of firefly luciferase was found to be modulated by both a chaperone molecule DnaK and the β(25−35) amyloid, but their effects were opposite in direction. The amyloid fibril drastically facilitated the luciferase aggregation, which may define a kind of anti-chaperone activity. The effect of the β(25−35) amyloid to promote protein aggregation and precipitation was further demonstrated for a wide variety of target proteins. The amount of coprecipitation was well correlated with the predicted isoelectric point of the target proteins, indicating that the interaction between the β(25−35) amyloid and the target was driven by an electrostatic force between them. This view was confirmed by the experiments using an electrically neutral mutant peptide, β(25−35)KA. It was also found that clustering of the β(25−35) peptide to form amyloid and the conformation of the target protein are additional factors that determine the strength of the amyloid−protein interaction. Spectroscopic and electron microscopic methods have revealed that the proteins coprecipitated with the β(25−35) amyloid formed amorphous aggregates deposited together with the amyloid fibrils. The conformation of protein molecules left in the residual soluble fraction was also damaged in the amyloid-containing solution. As a summary, this study has proposed a scheme for events related to the nonspecific amyloid−protein interaction, which may play substantial roles in in vivo conditions.

Much biochemical and biophysical research has focused its attention on protein aggregation events (*1*−*4*), partly motivated by the fact that deposit of a fibrous protein aggregate "amyloid" to biological tissues is often correlated with pathology of important human diseases (*5*−*8*). The amyloid is a special type of protein aggregate having a cross-β-fiber structure (*9*). Various types of proteins and peptides are known to form this type of aggregate, and the Alzheimer's β-amyloid peptide is one of the cases best investigated (*6*, *8*, *11*, *12*). Application of the β-amyloid peptide and its fragments to cultured cells and living tissues induces damage of their functions and viability (*13*−*15*). In vitro and in vivo analyses have suggested several microscopic mechanisms underlying the toxicity (*13*, *15*−*21*). The β-amyloid peptides are known to interact strongly with the lipid bilayer (*19*) and metal cations (*20*, *22*), which possibly initiate the cytotoxic events. Direct interactions of the β-amyloid peptides or its deposits with many proteins including acetylcholine esterase (*23*), apo-lipoprotein E (*24*), creatine phosphokinase, and glutamine synthetase (*25*) have also been found.

In surveying a pathological process in which an interaction between the amyloid and another protein might play a role, the research is usually motivated by a phenomenon concerning the dysfunction of a specific target protein. This often leads to our expectation that the mechanism of the interaction between the amyloid and the target is a very specific one. However, there is another possibility to be considered seriously that the amyloid fibril could strongly interact with proteins in a nonspecific manner. A wide range of soluble proteins in cytosol or extracelluar space may be absorbed on, precipitated with, or denatured by the amyloid. If this is really the case, deposit of the amyloid fibril will substantially alter the biological circumstances around the deposit with respect to protein composition. This could also play a substantial role in in vivo processes initiated by the amyloid. From this general point of view, further investigations of the interaction between the amyloid and proteins and conformational changes of the proteins following the interaction are of great importance.

We have presently surveyed the interaction of a wide range of soluble proteins with an amyloid fibril of β(25−35),[1] a cytotoxic fragment of the Alzheimer's β-peptide at positions 25−35 (*15*, *16*, *18*, *21*, *26*, *27*). This report begins with a part describing an effect of the β(25−35) amyloid on the aggregation rate of firefly luciferase by comparing with that

* Correspondence should be addressed to this author. Telephone: +81-776-61-8307, Fax: +81-776-61-8101, E-mail: konno@fmsrsa.fukui-med.ac.jp.

[1] Abbreviations: β(25−35), NH_2-GSNKGAIIGLM-COOH; β(25−35)KA, NH_2-GSNAGAIIGLM-COOH; β(25−35)NQ, NH_2-GSQKGAIIGLM-COOH; DTT, 1,4-dithiothreitol; EDTA, ethylenediaminetetraacetic acid; CD, circular dichroism; TEM, transmission electron microscopy; FT-IR, Fourier transform infrared spectroscopy; ThT, thioflavin T; CR, Congo red; MN, monellin; cyt c, cytochrome *c*; RNaseA, ribonuclease A; αLA, α-lactalbumin; Lyz, lysozyme; CaM, calmodulin; Mb, myoglobin; βLG, β-lactoglobulin; dPep, alkaline-denatured pepsin; CPK, creatine phosphokinase; Hb, hemoglobin; BSA, bovine serum albumin; Luc, firefly luciferase.

10.1021/bi002156h CCC: $20.00
Published on Web 01/25/2001

of a chaperone molecule, DnaK (*28*, *29*). In the following part, the amyloid-induced protein aggregation and its mechanisms are analyzed more generally utilizing various types of target proteins. Both mechanisms of the interaction and structures of the protein aggregates induced by the contact with the amyloid are investigated using several complementary methods. Based on the results, our present goal is to propose a scheme for the fate of proteins after exposure to the amyloid fibril.

EXPERIMENTAL PROCEDURES

Materials. A fragment of Alzheimer's β-peptide from the 25th to the 35th position, β(25−35) peptide (NH_2-GSNKGAIIGLM-COOH), and mutated peptides β(25−35)KA (NH_2-GSNAGAIIGLM-COOH) and β(25−35)NQ (NH_2-GSQKGAIIGLM-COOH) were synthesized, purified, and provided by Sawady Technology Co. (Tokyo, Japan). Horse heart cytochrome *c* (cyt c),[1] sperm whale myoglobin (Mb), bovine calmodulin (CaM), hen egg lysozyme (Lyz), human α-lactalbumin (αLA), bovine β-lactoglobulin A (βLG), bovine serum albumin (BSA), bovine ribonuclease A (RNaseA), monellin (MN), and porcine pepsin were purchased from Sigma Chemical Co. (St. Louis, Mo). Creatine phosphokinase (CPK) was purchased from Boehringer Manheim Co. (Manheim, Germany). Recombinant firefly luciferase (Luc) was purchased from Promega Co. (Madison, WI). DnaK was a kind gift of Dr. N. Tanaka (Kyoto Institute of Technology). Purity of all the proteins was checked by SDS−PAGE analysis. cyt c, Lyz, αLA, βLG, BSA, and pepsin were further purified by S-200 gel chromatography (Pharmacia, Sweden). Mb was purified by DE52 (Whatman) ion exchange chromatography. MN was purified as described by Fan et al. (*30*). CPK, Luc, and RNaseA were used without purification. Note that pepsin in the present experimental condition (pH 7.5) is in an alkaline-denatured state (dPep). Predicted isoelectric points of proteins were estimated using the program "Compute pI/Mw" on the web site http://www.expasy.ch/tools/pi_tool.html (*31*). Thioflavin T (ThT) and Congo red (CR) were purchased from Sigma Chemical Co. Other chemicals were of reagent grade and purchased from Nakalai Tesque Co. (Kyoto, Japan).

Preparation of Amyloid Solutions. Amyloid fibrils were prepared as follows. Powder of β(25−35) or β(25−35)KA was first dissolved in 50% acetonitrile and then lyophilized. The lyophilized peptide was redissolved in 10 mM Tris (pH 7.5) and 0.5 mM $CaCl_2$ at 1 mg/mL and incubated at 25 °C for 24 h. The amyloid formation was accelerated by seeding the solution with a small amount of mature amyloid fibrils. The sample was then centrifuged by a desktop micro-tube centrifugator at 15 000 rpm for 10 min, and the supernatant was carefully removed. The peptide concentration of the supernatant of β(25−35) was less than 0.02 mg/mL while that of β(25−35)KA was about 0.2 mg/mL (determined by the BCA method). The precipitant was resuspended just before use in 10 mM Tris (pH 7.5) and 0.5 mM $CaCl_2$ at a concentration of 1.0 mg/mL. The electron microscopic analysis of this sample confirmed formation of the amyloid fibril as shown later in Figure 6A for β(25−35). The solution of β(25−35)NQ peptide was prepared by dissolving the peptide powder in 10 mM Tris (pH 7.5) and 0.5 mM $CaCl_2$ at a concentration of 1.0 mg/mL, and a marginal amount of aggregates was removed by centrifugation.

Turbidity measurement. Turbidity of solutions containing Luc was monitored by absorbance at 320 nm. The solutions contained 0.13 mg/mL of Luc in 10 mM Tris (pH 7.5) and incubated at 25 °C. The measurements were done using a U-3300 spectrometer (Hitachi, Japan) under stirring. The path length of the sample cell was 10 mm. The absorbance change was normalized by its total change after incubation for 8 h.

Precipitation Experiments. The amyloid sample was mixed with various proteins in 10 mM Tris (pH 7.5) and 0.5 mM $CaCl_2$. Final concentrations of the amyloid fibril and an additional protein were 0.5 and 1.0 mg/mL, respectively. The solution of apo-αLA or partially reduced αLA additionally contained 2 mM EDTA or 2 mM DTT, respectively. Apo-αLA, a Ca^{2+}-free form of αLA, was used after incubation in the presence of EDTA for 6 h at 25 °C to ensure the removal of Ca^{2+} from αLA. Partially reduced αLA was also used after incubation in the presence of DTT for 6 h at 25 °C.

The sample mixtures above were incubated with stirring mildly at 25 °C for 8 h. As references, the protein solutions without the amyloid were incubated in parallel. Transmission electron microscopic analysis was done at this stage of the preparation. The samples were further centrifuged using a desktop centrifugator at 15 000 rpm for 30 min, and the supernatant was separated from the precipitant. The supernatant was subjected to determination of the protein concentration and the CD spectral measurement. The protein concentration was determined by the BCA method and the absorbance at 280 nm. The values obtained by the two methods were averaged for the final estimates. A calibration curve for the BCA method was prepared separately for each protein species. Absorbance was measured by a U-3300 spectrophotometer (Hitachi, Japan) using a quartz cell with a light path of 10 mm.

Fourier Transform Infrared Spectroscopy. A sample for the Fourier transform infrared (FT-IR) spectral measurement was prepared as follows. One milliliter of the sample of the precipitation experiment (after incubation for 8 h) was centrifuged by a desktop micro-tube centrifugator at 15 000 rpm for 15 min, and the supernatant was removed carefully. The precipitant was washed with 10 mM Tris (pH 7.5), and was precipitated again. The precipitant was dried up for 24 h in a vacuum incubator. The dry powder of the aggregates was enclosed in a KBr tablet by a conventional high-pressure method. The FT-IR spectrum of the samples was measured using a FT-730 spectrometer (Horiba, Japan).

Transmission Electron Microscopy. Electron micrographs of aggregates of amyloid and proteins were taken with a JEM-1200EX electron microscope (JEOL, Japan) operated at 100 kV, at a magnification of 40000×. The samples of mixtures of amyloid and proteins were applied to carbon grids and stained with 2% uranyl acetate. The images were recorded on FG electron microscopic films (Fuji film, Japan), developed in a D-19 developer (Kodak, USA) for 7 min, and digitized to 2048 × 2048 pixels by a SCAI precision scanner (Zeiss, Germany) at 7 μm step size.

ThT and Congo Red Binding Measurements. Sample solutions prepared for the coprecipitation experiments were diluted by 100 times with 10 mM Tris (pH 7.5) and 10 μM ThT or 5 μM CR for the dye binding experiments. Fluorescence spectra of ThT were measured with a F4500 fluorometer (Hitachi, Japan) using a quartz cell with a light path of

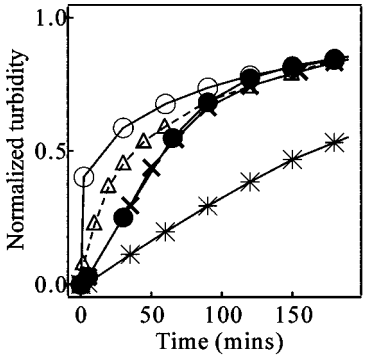

FIGURE 1: Kinetic changes in turbidity of firefly luciferase (0.13 mg/mL) in 10 mM Tris (pH 7.5) at 25 °C. (●) No additives. (∗) 0.1 mg/mL DnaK. (○) 0.05 mg/mL β(25−35) amyloid fibril. (△ with a dashed line) 0.05 mg/mL β(25−35)KA amyloid fibril. (×) 0.1 mg/mL BSA. Data obtained for the solutions containing additives without Luc were subtracted as a reference. The turbidity was normalized by the total change after a long enough (8 h) incubation time.

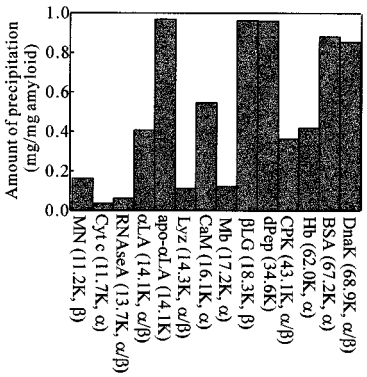

FIGURE 2: Amount of soluble proteins precipitated in the β(25−35) amyloid solution. Molecular weights and secondary structures of proteins are listed in parentheses, where α, β, and α/β are α-helix-rich, β-sheet-rich, and α/β types of secondary structure compositions, respectively. See footnote 1 for the abbreviations of proteins.

10 mm. The temperature of solutions was maintained at 25 °C by a thermostatically controlled water bath. The excitation wavelength was 440 nm, and bandwidths for excitation/emission lights were 5 nm/5 nm. Absorption spectra of CR were taken with a U-3300 spectrophotometer (Hitachi, Japan).

Circular Dichroism Measurement. Circular dichroism (CD) spectra in the far-UV region were measured with a Jasco J-720 WI spectropolarimeter (Jasco, Japan) using quartz cells with a light path of 1 mm. The temperature of the solutions was controlled by a JASCO temperature controller within ±0.1 °C.

Enzyme Activity Assays. The kinase activity of CPK was determined using the CPK assay kit of Sigma Chemical Co. The nuclease activity of RNaseA was determined by mixing an aliquot of the RNaseA sample with tRNA solution (10 mM Tris, pH 7.5). After an adequate incubation time at 37 °C, the amount of digested tRNA was measured by agarose gel electrophoresis followed by densitometric analysis. The activity of Luc was determined using the Luciferase Assay System of Promega Co.

RESULTS

Effects of β(25−35) Amyloid on the Aggregation Rate of Luc. Firefly luciferase (Luc) has been a good model protein for studying chaperone-assisted protein folding. A combination of several chaperone molecules including DnaK suppresses aggregation of Luc in its partially denatured states, and assists its proper folding (*28*, *29*). On the other hand, Luc loses its activity by forming aggregates and precipitants even in its native condition. Filled circles in Figure 1 show the time course of this aggregation of Luc at pH 7.5 and 25 °C monitored by turbidity. Its time constant was about 1 h, and after incubation for several hours nominally all the Luc molecules could be removed from solution by a brief centrifugation. The activity loss of Luc occurs almost in parallel with the aggregation (data not shown). We found that DnaK alone could have a substantial effect to retard this aggregation of Luc (stars in Figure 1). This is interesting because combined usage of DnaK, DnaJ, GrpE, ATP, etc. is usually required for its chaperone activity to assist proper folding of denatured proteins (*28*, *29*, *32*). Other proteins such as BSA and lysozyme did not have the activity to retard Luc aggregation (crosses in Figure 1 for BSA). Since our present focus is on phenomena related to the amyloid, no more details are shown on the DnaK activity found here. In contrast to the effect of DnaK, addition of the β(25−35) amyloid to the Luc solution strongly facilitated the aggregation of Luc (open circles in Figure 1). The turbidity of the solution quickly increased within a few minutes, followed by a minor slower component. The effect of the amyloid to facilitate protein aggregation is opposite in direction to that of DnaK. This may be a kind of anti-chaperone activity (*33*, *34*). The data trace for mutant β(25−35)KA amyloid in Figure 1 (triangles) fell in an intermediate range between those of Luc with and without β(25−35) amyloid, which we will explain later.

Precipitation of Various Soluble Proteins with β-Amyloid-(25−35). To see whether the effect of the β(25−35) amyloid to facilitate protein aggregation is a general phenomenon, various types of soluble proteins were coincubated with the β(25−35) amyloid fibril at pH 7.5 and 25 °C for 8 h, and then the protein concentration in the supernatant of the samples were determined (Figure 2). Those target proteins had no intrinsic tendency to form aggregates in the solution without the amyloid. The result showed that the amount of proteins coprecipitated with the amyloid varied widely depending on protein species (Figure 2).

Mechanism of the Interaction between the Amyloid and Proteins. Physical mechanisms of the interaction between the amyloid and soluble proteins were investigated for three different possibilities of contributions; those are: (1) electrostatic interaction, (2) clustering of the β(25−35) peptide to form amyloid, and (3) conformation of target proteins.

Either the molecular weight or the secondary structure composition of soluble proteins was not correlated with the amount of their coprecipitation with the amyloid (Figure 2). A better correlation was found for the predicted isoelectric point of the proteins (the linear correlation coefficient being −0.86; Figure 3A). This suggests that the interactions between the amyloid and soluble proteins are at least partly governed by charge−charge interactions. The β(25−35) peptide has only one charged side chain on Lys28, and thus the β(25−35) amyloid fibril must have a net positive charge at neutral pH. It is plausible that the positive charges on

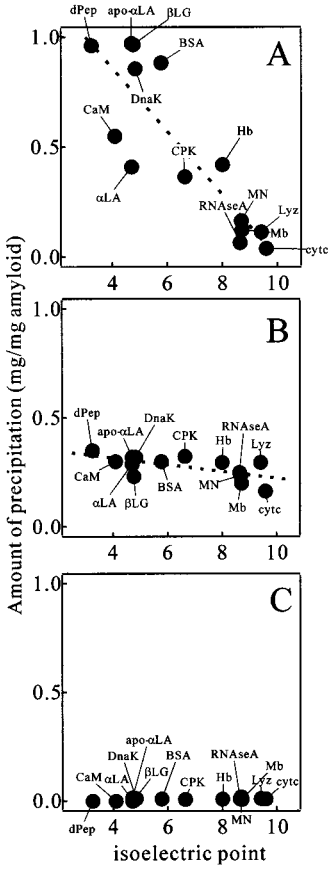

FIGURE 3: Amount of precipitation of proteins induced by β(25−35) (A), β(25−35)KA (B), and β(25−35)NQ (C) plotted against the predicted isoelectric points of the proteins. Dashed lines are linearly fitted lines. The predicted isoelectric points of proteins were 8.68 (MN), 9.59 (cyt c), 8.64 (RNaseA), 4.70 (αLA), 9.41 (Lyz), 4.09 (CaM), 8.71 (Mb), 4.76 (βLG), 3.24 (pepsin), 6.63 (CPK), 8.00 (Hb), 5.77 (BSA), and 4.83 (DnaK). See Experimental Procedures for the prediction method and footnote 1 for the abbreviations of proteins.

Lys28 clustered on the amyloid attract negative charges on an acidic protein to form a complex. To provide evidence for this electrostatic interpretation, the precipitation experiment was conducted using the amyloid fibril formed by mutant peptide β(25−35)KA, in which Lys28 of β(25−35) was mutated to Ala28 (*35*). The TEM analysis has found that the β(25−35)KA peptide forms regular fibrils (data not shown). The result showed that the amount of coprecipitation induced by β(25−35)KA was around 0.3 mg (per 1 mg of amyloid) for all the protein species, and not a significant function of the predicted isoelectric point (Figure 3B). We conclude that the electrostatic force exerted between positive charges on the β(25−35) fibril and negative charges on acidic proteins strongly promoted the precipitation of the acidic proteins. This view is also supported by the fact that the β(25−35)KA amyloid accelerated the aggregation of Luc significantly to a less extent than that of β(25−35) (Figure 1).

Another mutant peptide, β(25−35)NQ, in which Asn29 was mutated to Gln28, was also tested to see whether the aggregated form of the β(25−35) peptide is necessary for the induction of protein aggregation and precipitation. Although this mutant is conservative with respect to charge composition, it did not form a significant amount of amyloid aggregates even after incubation for 24 h in our preparation

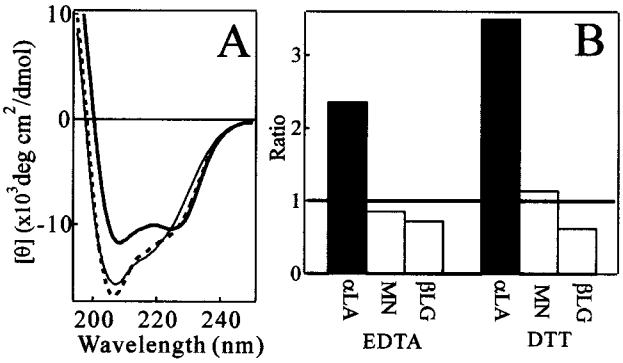

FIGURE 4: (A) Far-UV CD spectra of αLA without amyloid, demonstrating partial unfolding of αLA by addition of EDTA or DTT. Boldface line: no additive. Thin line: 2 mM EDTA (apo-αLA). Dashed line: 2 mM DTT (partially reduced αLA). (B) Ratios of the amount of the amyloid-induced precipitation of αLA, MN, and βLG in the presence of 2 mM EDTA (labeled as "EDTA") or 2 mM DTT (labeled as "DTT"). The ratios were calculated by referring to the values obtained without the additives.

(checked by determining the peptide concentration in the supernatant and ThT binding). By mixing various protein solutions with this soluble mutant peptide, we performed precipitation experiments in the same way as those described above, but no protein coprecipitated after incubation for 8 h (Figure 3C). Comparison of this result with those of β(25−35) has indicated clustering of the amyloid peptide is necessary to induce the aggregation of the proteins.

To examine the effect of conformational changes of the target protein on its aggregation induced by the amyloid, special attention was focused on αLA. At neutral pH, αLA in the Ca^{2+}-bound form has a rigidly folded conformation, but removal of the Ca^{2+} ions by EDTA transforms the conformation to a well-established compact denatured state, "molten globule" (*36*, *37*). Furthermore, disulfide bridges of the folded αLA can be reduced partially by adding DTT to the αLA solution, which also produces a partially unfolded conformation of αLA. Far-UV CD spectra of αLA in Figure 4A typically shows the partial unfolding of αLA by incubation with small amounts of EDTA or DTT (Figure 4A). This addition of EDTA (apo-αLA) or DTT (partially reduced αLA) drastically enhanced the coprecipitation of αLA with the β(25−35) amyloid (Figure 4B). The results of αLA were in clear contrast with the other reference cases such as MN and βLG (Figure 4B), whose CD spectra demonstrated little change of their conformations by the addition of EDTA and DTT (data not shown). In all of the results, the interaction between the amyloid and αLA was enhanced strongly by the partial unfolding of αLA.

Structures of the Amyloid-Induced Protein Aggregates. Although we resuspended the coprecipitants of the amyloid and proteins in a buffer solution and tried to redissolve the protein aggregates, they could not be recovered substantially (as determined by the absorption and the BCA method). This means that the protein stuck to the amyloid very strongly or formed practically insoluble aggregates. The secondary structure composition of the coprecipitants of the amyloid and proteins was analyzed by FT-IR spectroscopy (Figure 5A). The amide I band of the β(25−35) amyloid alone had peaks at 1632 and 1672 cm^{-1} (top of Figure 5A), typical for the antiparallel β-sheet structure of amyloid fibrils (*38*). The spectra of the precipitants formed by adding proteins such

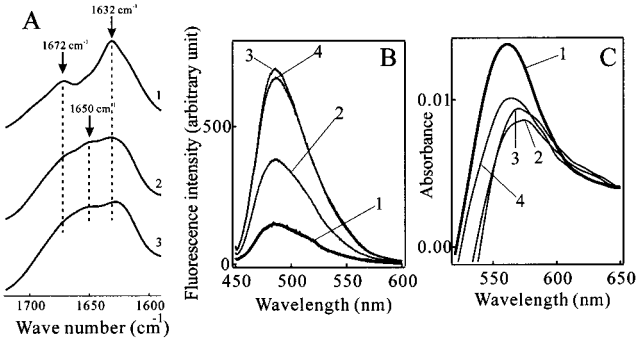

FIGURE 5: (A) FT-IR spectra of aggregates of β(25−35) (top, 1), β(25−35)+βLG (middle, 2), and β(25−35)+apo-αLA (bottom, 3). (B) ThT fluorescence spectra excited at 440 nm and (C) CR difference absorption spectra for the samples of β(25−35) (line 1), β(25−35)+αLA (line 2), β(25−35)+apo-αLA (line 3), and β(25−35)+pepsin (line 4). The difference spectra in (C) were obtained by subtracting the spectra of the CR solution without the amyloid fibril.

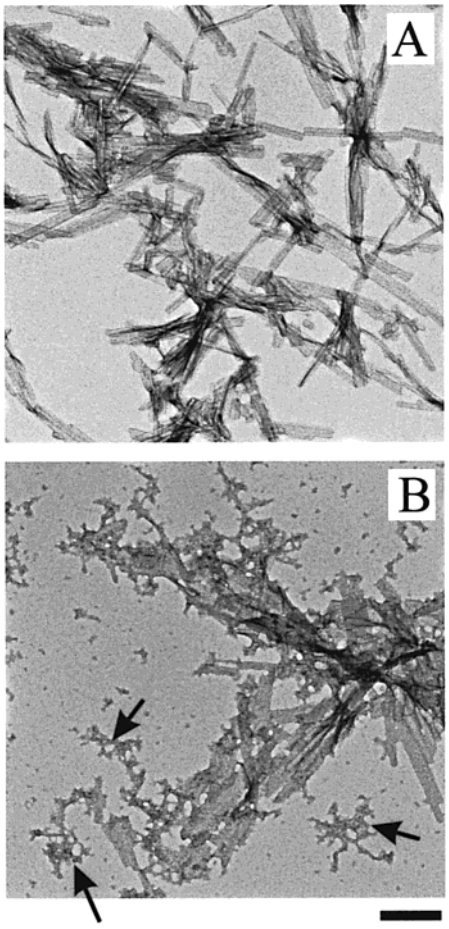

FIGURE 6: Negatively stained TEM images for β(25−35) (A) and β(25−35)+apo-αLA (B). Bar = 200 nm.

as βLG and apo-αLA (middle and bottom of Figure 5A) had an additional band at around 1650 cm^{-1}, which can be assigned to non-β-sheet structures (*39*). Morphology of the precipitants was characterized by negatively stained transmission electron microscopy (TEM). The β(25−35) peptide alone formed amyloid fibrils with a width of 20−40 nm (Figure 6A). Addition of cyt c or Mb, which precipitated only marginally in the amyloid solution (Figure 2), did not substantially alter the look of the TEM image. However, the coprecipitation of proteins such as βLG and apo-αLA altered

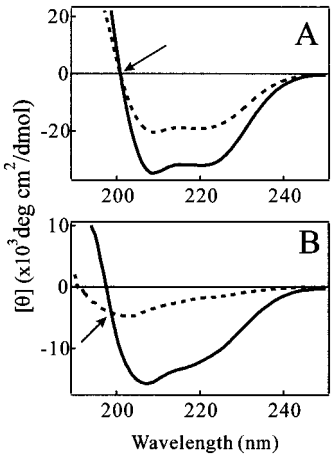

FIGURE 7: Far-UV CD spectra of the supernatant of the samples of the precipitation experiments for BSA (A) and partially reduced αLA (B). Dashed lines: incubated with the β(25−35) amyloid. Solid lines: incubated without the amyloid. Arrows: isodichroic points of two spectra.

the appearance of the image (Figure 6B for apo-αLA). A regular impression of the amyloid fibrils was damaged by deposition of amorphous materials on the fibrils. A substantial amount of the amorphous aggregates was also observed without attaching to the fibrils (arrows in Figure 6B). The results of TEM and FT-IR demonstrated that protein molecules that interacted with the β(25−35) amyloid formed amorphous aggregates and deposited together with the amyloid fibrils. More extensive spectroscopic and microscopic analyses using a better experimental condition must be done in future studies to detail the conformational changes of the soluble proteins contacting the amyloid.

Some diagnostic methods for detecting amyloid monitor binding of several dyes using spectroscopic methods. Thioflavin T (ThT) is a fluorescence dye that strongly binds to amyloid accompanied with a fluorescence enhancement (*40*). We found that the fluorescence intensity of ThT in the amyloid solution was markedly increased by the coprecipitation of soluble proteins almost in parallel with the amount of the coprecipitation (Figure 5B; see also Figure 2). One of its possible interpretations is that the adhesion of proteins on the surface of the amyloid increased the number of dye binding sites, or, alternatively, increased the hydrophobicity of the environment around the binding sites. Congo red (CR) is another dye diagnostic of amyloid (*41*). Binding of CR monitored by the absorption spectral measurement was suppressed when proteins coprecipitated with the amyloid (Figure 5C). This implies that the adhesion of the coprecipitants to the amyloid surface prevent CR from its binding to the binding sites. The ThT and CR binding experiments supported that the coprecipitated protein adheres on the amyloid and modifies its surface properties substantially.

Structure of Proteins in the Residual Soluble Fraction. The far-UV CD spectra of proteins in the supernatant fraction of the sample used in the precipitation experiments with and without the β(25−35) amyloid fibril were measured to compare the protein conformation in the residual soluble fractions (Figure 7). The vertical scale of the spectra in Figure 7 was calculated using the total protein concentration, and thus the smaller signal intensity of the sample incubated with the amyloid than that without it could be explained by the amyloid-induced coprecipitation. However, if the conforma-

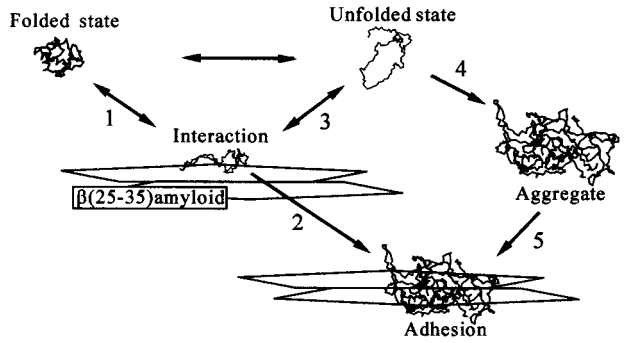

FIGURE 8: Hypothetical scheme of events following the interaction between the β(25−35) amyloid fibrils and soluble proteins.

tion of the protein in the supernatant fraction is the same for both the samples with and without the amyloid, the shape of the spectra should not be changed, and an isodichroic point of the two spectra (arrows in Figure 7) should reside exactly on the horizontal zero axis. This was really the case for some proteins such as BSA and βLG (Figure 7A for BSA), indicating that the conformation of these proteins in the supernatant fraction was not affected by the presence of the amyloid. However, for some proteins such as MN, apo-αLA, and partially reduced αLA in the amyloid solution, substantial spectral change occurred in the direction of reducing the secondary structure content (Figure 7B for partially reduced αLA). At least for some protein species, the conformation in the nonprecipitated fraction was also damaged by their interaction with the amyloid (Figure 7B).

DISCUSSION

Proposed Scheme for β(25−35) Amyloid−Protein Interaction. This study is a collection of phenomena related to the interaction between the β(25−35) amyloid fibril and soluble proteins. Based on it, we propose a scheme for a series of events following the interaction (Figure 8). Our main conclusion is that a wide range of soluble proteins strongly interacts with the β(25−35) amyloid (step 1 in Figure 8). Following this interaction, the protein forms the amorphous aggregates and deposits together with the amyloid fibril (step 2 of Figure 8). The amyloid also destroys the conformation of the protein in the residual soluble fraction (Figure 7B). The interaction between the amyloid and proteins probably exerts a force to unfold the protein conformation on the surface of the amyloid fibril (step 3 of Figure 8). This amyloid-induced unfolding (or partial unfolding) is a probable event that initiates the aggregation and the precipitation of the protein (steps 4−5 of Figure 8) since the protein in an unfolded conformation has much stronger tendency to aggregate than that in the folded conformation (*2*, *3*). The (partial) unfolding after the contact with the amyloid would also cause a strong adhesion of this protein molecule on the amyloid fibril, as supported by the results for αLA in Figure 4. A stepwise accumulation of the (partially) unfolded protein molecules on the surface of the amyloid may be another origin of the formation of the large aggregates around the fibrils (step 2 of Figure 8). In summary, the β(25−35) amyloid fibril has the ability to destroy the native conformation of a protein and induce its aggregation and deposition. These functions of the amyloid fibril are opposite in direction to those of the chaperone system such as those composed of Hsp70, GroEL and DnaK, etc., which assists protein folding in its biosynthesis and suppresses in vivo protein aggregation (*42*−*44*). The opposite direction of the effects is clearly presented in Figure 1 of this study. In a limited sense, the β(25−35) amyloid fibril is anti-chaperone. This term was previously used by Ostermeier et al. (1996) for the activity of a disulfide isomerase that facilitates the misfolding and aggregation of its substrates (*33*). It should be noted here that the scheme of Figure 8 was proposed only for a certain range of proteins, and does not imply that all the proteins should follow this mechanism.

Physical Determinants of β(25−35) Amyloid−Protein Interaction. One of the attractive forces acting between the β(25−35) amyloid and a soluble protein was found to be electrostatic (Figure 3A,B). The electrostatic force originated from the β(25−35) peptide is also known to be the physical origin of the interaction between this peptide and lipid membranes (*27*, *45*). The composition of charged residues of amyloid-forming proteins and peptides could be one of the general factors that determine their pathological potentials. Another determinant of the interaction was the amyloid-like assembly of the amyloid peptides (Figure 3), suggesting that clustering of the charged sites of the β(25−35) peptide is required to induce protein aggregation. On the other hand, the exposure of the internal core of a soluble protein by its partial unfolding strongly promoted the amyloid−protein interaction (Figure 4A). A large contact area between the amyloid and the partially unfolded protein would contribute importantly to their interaction. Since the partial unfolding of protein exposes the hydrophobic parts of the protein very much (*36*, *37*), the hydrophobic interaction between the protein and the surface of the amyloid may also contribute to the interaction. In fact, the amount of coprecipitation of proteins with the electrically neutral β(25−35)KA fibrils was more than negligible (Figure 3B), supporting that thermodynamic forces other than the electrostatic one also play significant roles in the interaction. It is also notworthy that a good correlation between the isoelectric point and the amount of precipitation in Figure 3A was found for the protein samples of the same protein concentration in units of milligrams per milliliter. This indicates that the molar concentration of the protein in solution is of minor importance for the precipitation phenomenon. It may suggest that the aggregation event occurs on the surface of the amyloid fibril, not in the solution phase.

Physiological Implications. This report has shown that amyloid fibrils have the potential to interact with proteins nonspecifically. It may imply that the interaction between the amyloid and proteins could damage a wide range of biological systems not only in a specific manner but also in a nonspecific process. Removal of a wide range of enzymes in the cell as well as in the extracellular matrix could affect the functions of cells and organs. For example, inactivation of CPK by the β(25−35) peptide has previously been explained by radical formation on the peptide (*19*), but the present report found another nonspecific origin for the interaction between CPK and β(25−35) (Figure 2). Recent studies suggested that the β-amyloid is toxic in its protofilament stage and the mature fibril is less toxic (*46*). However, precise pathological roles of the amyloid in damaged tissues or cells are largely unsolved yet, and deposition of amyloid fibrils still remains a candidate of toxic origins. Nonspecific processes similar to those in Figure 8 may also be driven by

the amyloid in the protofilament stage, although the present conclusion should be limited to the case of the matured amyloid. The precipitation of soluble proteins around the amyloid increases the absolute volume of deposited aggregates, which could be another nonspecific origin of the amyloid toxicity. On the other hand, we should also consider the possibility that the coprecipitation of protein with the amyloid fibril has a physiological role in an opposite direction. As seen by the results of the CR binding (Figure 5C), adhesion of the aggregated proteins on the surface of the amyloid substantially alters the surface properties of the amyloid. This may hide toxic sites of the amyloid, and result in loss of its cytotoxicity.

When the amyloid interacts with proteins in a nonspecific manner, the target proteins to be absorbed on the amyloid would vary depending on the location of its deposition. In addition, although the β(25−35) amyloid has a net positive charge at neutral pH and thus interacted preferably with acidic proteins, a different type of amyloid may have a different type of protein selectivity. The in vivo processes initiated by the amyloid deposit could depend on both the species of amyloid and the location of its deposition. For example, the proteins we examined here included the chaperone protein DnaK, which precipitated very strongly in the amyloid solution (Figure 2). Deposit of amyloid in the vicinity of the chaperone system in living cells could damage it. Furthermore, the strong affinity of the amyloid to partially unfolded proteins (Figure 4) could also compete with the function of the chaperone in protein biosynthesis or in recovery from damage. These considerations may encourage further analyses of the amyloid−chaperone interactions in in vivo conditions.

ACKNOWLEDGMENT

I thank Dr. K. Nagayama, Dr. S. Oiki, Dr. H Naiki, and Dr. Y. Kamatari for their helpful discussions and suggestions throughout this work. I also thank Dr. N. Tanaka for his kind gift of purified DnaK.

REFERENCES

1. Clark, A., Judge, F. J., Richards, J. B., Stubbs, J. M., and Suggett, A. (1981) *Int. J. Pept. Protein Res. 17*, 380−392.
2. Jaenick, R., and Seckler, R. (1997) *Adv. Protein Chem. 50*, 1−59.
3. Fink, A. (1998) *Folding Des. 3*, R9−23.
4. Dobson, C. M. (1999) *Trends Biol. Chem. 24*, 329−332.
5. Sipe, J. D. (1992) *Annu. Rev. Biochem. 61*, 947−975.
6. Tan, S. Y., and Pepys, M. B. (1994) *Histopathology 25*, 403−414.
7. Prusiner, S. B., Scott, M. R., DeArmond, S. J., and Cohen, F. E. (1998) *Cell 93*, 337−348.
8. Koo, E. H., Lansbury, P. T., Jr., and Kelly, J. W. (1999) *Proc. Natl. Acad. Sci. U.S.A. 96*, 9989−9990.
9. Sunde, M., and Blake, C. (1997) *Adv. Protein Chem. 50*, 123−159.
10. Harper, J. D., and Lansbury, P. T., Jr. (1997) *Annu. Rev. Biochem. 66*, 385−407.
11. Kelly, J. W. (1998) *Curr. Opin. Struct. Biol. 8*, 101−106.
12. Rochet, J.-C., and Lansbury, P. T., Jr. (2000) *Curr. Opin. Struct. Biol. 10*, 60−68.
13. Yankner, B. A., Dawes, L. R., Fisher, S., Villa-Komaroff, L., Oster-Granite, M. L., and Neve, R. L. (1989) *Science 245*, 417−420.
14. Pike, C. J., Burdick, D., Walencewicz, A. J., Glabe, C. G., and Cotman, C. W. (1993) *J. Neurosci. 13*, 1676−1687.
15. Shearman, M. S., Ragan, C. I., and Iversen, L. L. (1994) *Proc. Natl. Acad. Sci. U.S.A. 91*, 1470−1474.
16. Meda, L., Cassatella, M. A., Szendrei, G. I., Otvos, L., Jr., Baron, P., Villalba, M., Ferrari, D., and Rossi, F. (1995) *Nature 374*, 647−650.
17. Schubert, D., Behl, C., Lesley, R., Brack, A., Dargusch, R., Sagara, Y., and Kimura, H. (1995) *Proc. Natl. Acad. Sci. U.S.A. 92*, 1989−1993.
18. Suh, Y. H., Chong, Y. H., Kim, S. H., Choi, W., Min, K., Jeong, S. J., Fraser, S. P., and Djamgoz, M. B. (1996) *Ann. N.Y. Acad. Sci. 786*, 169−183.
19. Hertel, C., Terzi, E., Hauser, N., Jakob-Rotne, R., Seelig, J., and Kemp, J. (1997) *Proc. Natl. Acad. Sci. U.S.A. 94*, 9412−9416.
20. Atwood, C. S., Moir, R. D., Huang, X., Scarpa, R. C., Bacarra, N. M., Romano, D. M., Hartshorn, M. A., Tanzi, R. E., and Bush, A. I. (1998) *J. Biol. Chem. 273*, 12817−12826.
21. Bianca, V. D., Dusi, S., Bianchini, E., Dal Pra, I., and Rossi, F. (1999) *J. Biol. Chem. 274*, 15493−15499.
22. Terzi, E., Holzemann, G., and Seelig, J. (1997) *Biochemistry 36*, 14845−14852.
23. Inestrosa, N. C., Alvarez, A., Perez, C. A., Moreno, R. D., Vicente, M., Linker, C., Casanueva, O. I., Soto, C., and Garrido, J. (1996) *Neuron 16*, 881−891.
24. Naiki, H., Hasegawa, K., Yamaguchi, I., Nakamura, H., Gejyo, F., and Nakakuki, K. (1998) *Biochemistry 37*, 17882−17889.
25. Hensley, K., Carney, J. M., Mattson, M. P., Aksenova, M., Harris, M., Wu, J. F., Floyd, R. A., and Butterfield, D. A. (1994) *Proc. Natl. Acad. Sci. U.S.A. 91*, 3270−3274.
26. Yankner, B. A., Duffy, L. K., and Kirschner, D. A. (1990) *Science 250*, 279−282.
27. Hertel, C., Terzi, E., Hauser, N., Jakob-Rotne, R., Seelig, J., and Kemp, J. (1997) *Proc. Natl. Acad. Sci. U.S.A. 94*, 9412−9416.
28. Schroder, H., Langer, T., Hartl, F. U., and Bukau, B. (1993) *EMBO J. 12*, 4137−4144.
29. Buchberger, A., Valencia, A., McMacken, R., Sander, C., and Bukau, B. (1994) *EMBO J. 13*, 1687−1695.
30. Fan, P., Bracken, C., and Baum, J. (1993) *Biochemistry 32*, 1573−1582.
31. Bjellqvist, B., Hughes, G. J., Pasquali, C., Paquet, N., Ravier, F., Sanchez, J. C., Frutiger, S., and Hochstrasser, D. (1993) *Electrophoresis 14*, 1023−1031.
32. Langer, T., Lu, C., Echols, H., Flanagan, J., Hayer, M. K., and Hartl, F. U. (1992) *Nature 356*, 683−689.
33. Ostermeier, M., De Sutter, K., and Georgiou, G. (1996) *J. Biol. Chem. 271*, 10616−10622.
34. Sideraki, V., and Gilbert, H. F. (2000) *Biochemistry 39*, 1180−1188.
35. Sato, K., Wakamiya, A., Maeda, T., Noguchi, K., Takashima, A., and Imahori, K. (1995) *J. Biochem. (Tokyo) 118*, 1108−1111.
36. Kuwajima, K. (1989) *Proteins: Struct., Funct., Genet. 6*, 87−103.
37. Ptitsyn, O. B. (1995) *Curr. Opin. Struct. Biol. 5*, 74−78.
38. Halverson, K. J., Sucholeiki, I., Ashburn, T. T., and Lansbury, P. T., Jr. (1991) *J. Am. Chem. Soc. 113*, 6701−6703.
39. Surewicz, W. K., Mantsch, H. H., and Chapman, D. (1993) *Biochemstry 32*, 389−394.
40. Naiki, H., Higuchi, K., Hosokawa, M., and Takeda, T. (1989) *Anal. Biochem. 177*, 244−249.
41. Klunk, W. E., Pettegrew, J. W., and Abraham, D. J. (1989) *J. Histochem. Cytochem. 37*, 1273−1281.
42. Martin, J., and Hartl, F. U. (1997) *Curr. Opin. Struct. Biol. 7*, 41−52.
43. Braig, K. (1998) *Curr. Opin. Struct. Biol. 8*, 159−165.
44. Ellis, R. J., and van der Vies, S. M. (1991) *Annu. Rev. Biochem. 60*, 321−347.
45. Terzi, E., Holzemann, G., and Seelig, J. (1994) *Biochemistry 33*, 7434−7441.
46. Lansbury, P. T., Jr. (1999) *Proc. Natl. Acad. Sci. U.S.A. 96*, 3342−3344.

BI002156H